**Supplementary material for:**
**High-pressure studies of charge density wave state of Rare-Earth Tritellurides by Raman spectroscopy**

Jan Kopaczek[1,2 a)], Han Li[1], Kentaro Yumigeta[1], Renee Sailus[1], Mohammed Y. Sayyad[1], Seyed Tohid Rajaei Moosavy[1], Robert Kudrawiec[2], and Sefaattin Tongay[1]
[1] Materials Science and Engineering, School for Engineering of Matter, Transport and Energy, Arizona State University, Tempe, Arizona 85287, USA
[2] Department of Semiconductor Materials Engineering, Faculty of Fundamental Problems of Technology, Wroclaw University of Science and Technology, Wybrzeże Wyspiańskiego 27, 50-370 Wrocław, Poland
[a)] Corresponding author: jan.kopaczek@pwr.edu.pl and sefaattin.tongay@asu.edu

## I. Pressure-dependent Raman spectra for $RTe_3$ (R = La, Ce, Pr, Sm, Gd, and Tb)

Here, we are comparing XRD reflection positions between experimentally obtained values (based on the Lorentz fitting procedure) and theoretically predicted (from the International Centre for Diffraction Data). A good agreement between them can be observed for studied single-crystalline samples.

Table T1. Comparison of experimentally and theoretically obtained XRD reflections for $NdTe_3$ crystal.

| XRD reflection | Obtained experimentally (º) | Predicted theoretically (º) |
|---|---|---|
| (060) | 20.6105 | 20.59038 |
| (080) | 27.59529 | 27.57152 |
| (0120) | 41.92169 | 41.88592 |
| (0140) | 49.33485 | 49.29212 |
| (0160) | 56.97585 | |

In figure S1, we have displayed XRD spectra for all studied in our work materials, including $NdTe_3$, for which spectrum is also presented in the main text in Fig. 1. As R lanthanide metal cation increases (i.e., larger 4f electron number), the XRD reflection shifts to higher values (inset of figure S1), corresponding to lattice constant reduction.

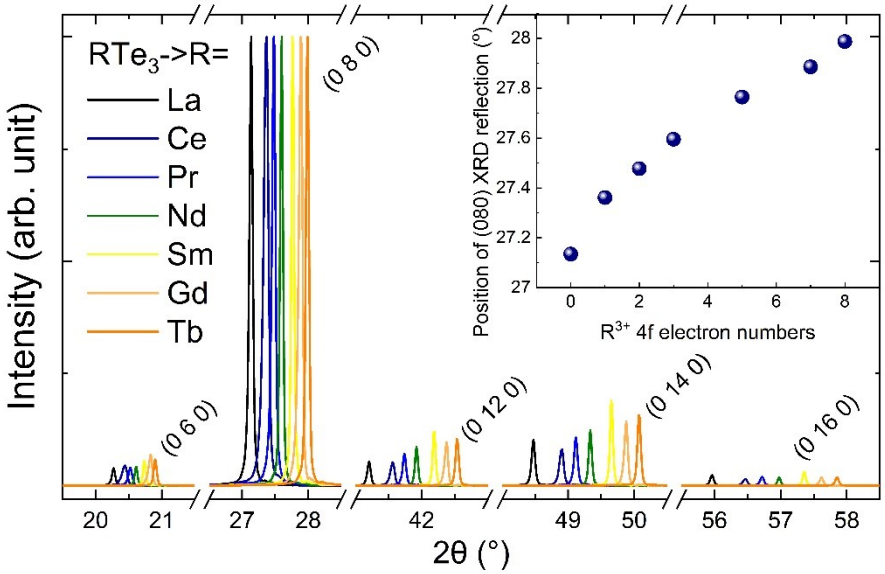


Figure. S1 XRD spectra for all studied crystals. The inset shows the position of (080) reflection in the function of R3+ 4f electron numbers.

To identify and assign CDW-related amplitude mode and couple with it phonon mode, we have performed measurements of Raman spectra in a broad temperature range, from 79 to 463 K. It can be clearly observed that the position of phonon ($A_g$) mode and amplitude mode at respectively ~56 $cm^{-1}$ and ~75 $cm^{-1}$ (at low temperature) display anticrossing behavior as shown with a dashed line in Fig. S2a. Moreover, we have shown that in the temperature range between 298 and 388 K, these two modes interchange their intensity Fig. S2b; at 358 K (green spectra), they share the same intensity. To clearly show that behavior, we have displayed individual mode by fitting experimental spectra with two Lorentz functions (dotted lines) Fig. S2b. Additionally, at 358 K, both modes change their nature, i.e., the low-frequency mode is phononic in nature, and high frequency one resemblance amplitude mode, whereas above 358 K, Raman mode at ~52 $cm^{-1}$ becomes amplitude mode and another one (at ~60 $cm^{-1}$) has phononic nature. It can be seen in Fig. S2a that phonon mode (gray dashed line) is less sensitive to temperature. Such evolution of modes with temperature was previously reported, and its characteristics for materials that can exist in the CDW phase in which phonon mode couples to amplitude mode, leading to anticrossing behavior. [1–3]

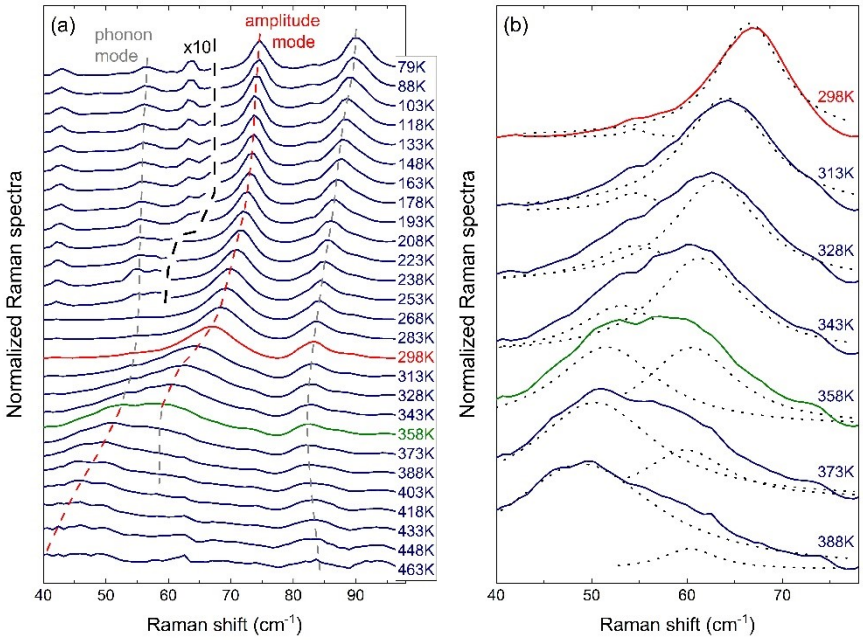


Figure S2. (a) Temperature dependency of Raman spectra obtained for $NdTe_3$ crystal (dashed lines are added as an eye guide). (b) Detailed presentation of spectra in the range from 298 to 388 K displaying the evolution of the intensity of phonon and amplitude mode. The dotted line represents the result of the Lorentz fitting procedure.

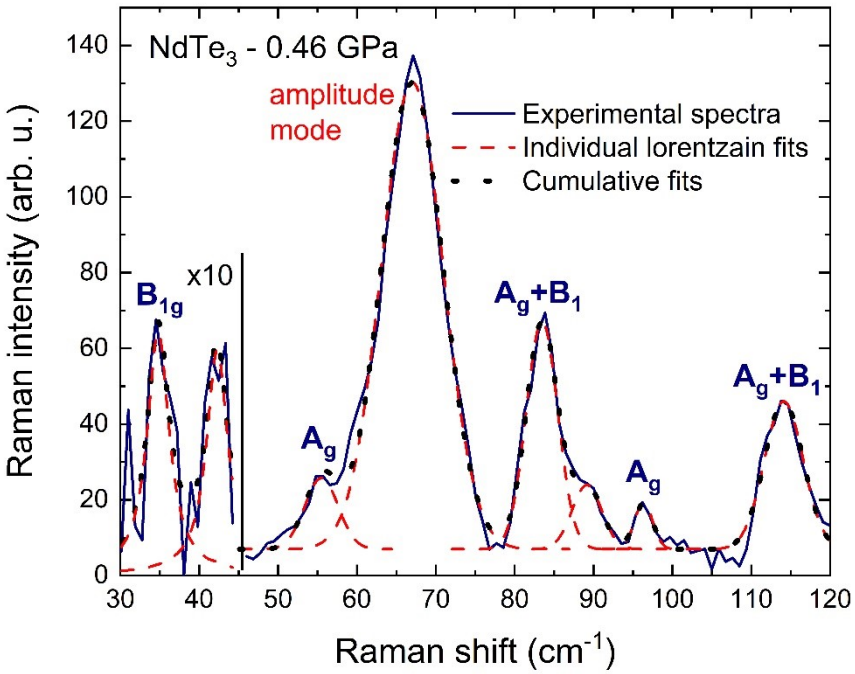


Figure S3. Exemplary results of Lorentz fitting procedure performed for Raman spectra obtained for $NdTe_3$ crystal at 0.46 GPa.

Below, we present the results of Raman spectra measurements with hydrostatic pressure performed for the remaining crystals studied in our work. Moreover, regarding plots showing the position of each mode in the function of pressure, we have displayed all the modes obtained in the results of the fitting procedure. Based on this analysis, the pressure value at which each of these crystals undergoes the transition from CDW to non-CDW phase was obtained. In Fig. S8, presenting results of studies for $GdTe_3$ crystals, we marked with an olive dotted line Raman peak related to the oxidation process (detailed analysis of that process will be the subject of another work).

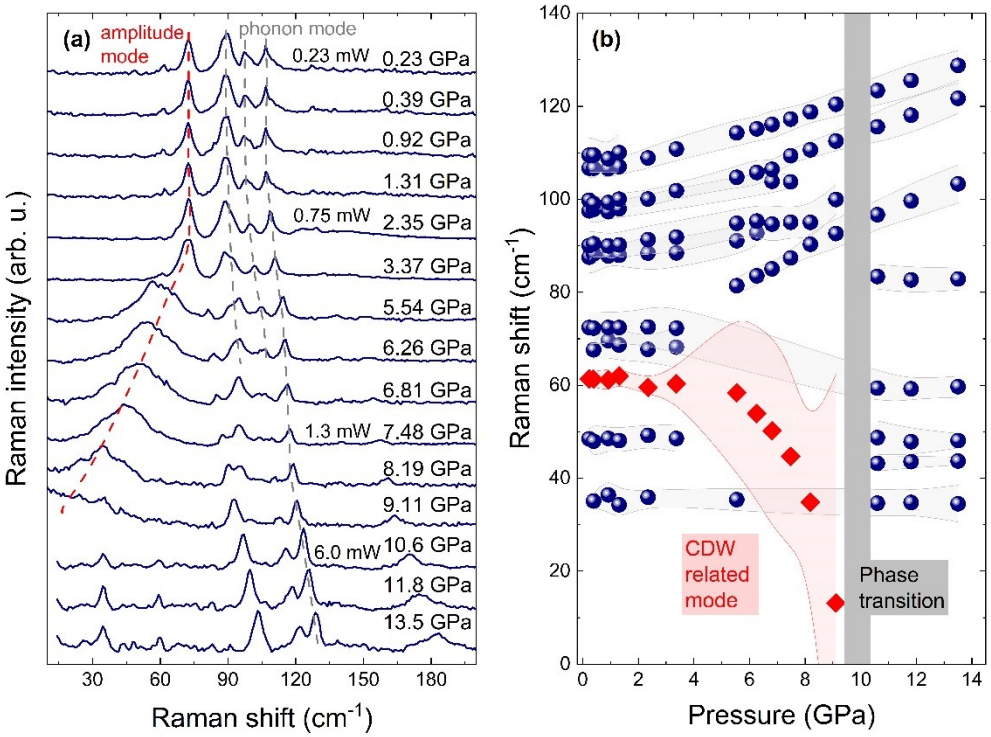


Figure S4. (a) Pressure-dependent Raman spectra obtained for $LaTe_3$ crystal (dashed lines are added as an eye guide). (b) Position of a phonon (navy points) and amplitude (red diamonds) mode in the function of pressure obtained with Lorentz fitting procedure – the shaded area represents broadening of each Raman mode.

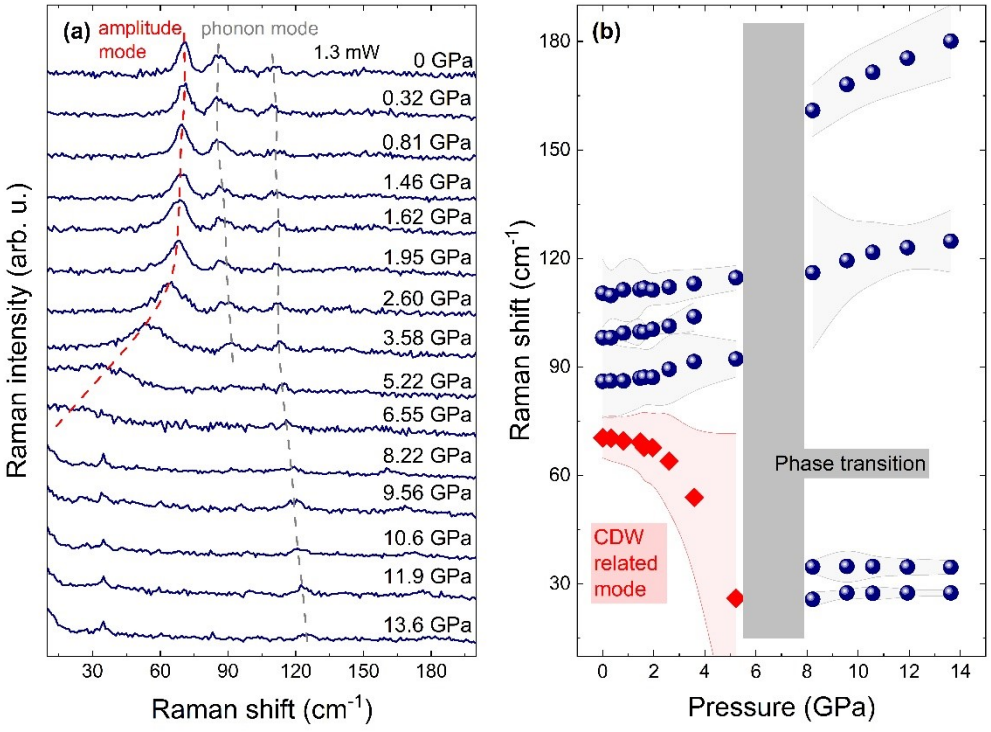


Figure S5. (a) Pressure-dependent Raman spectra obtained for $CeTe_3$ crystal (dashed lines are added as an eye guide). (b) Position of a phonon (navy points) and amplitude (red diamonds) mode in the function of pressure obtained with Lorentz fitting procedure – the shaded area represents broadening of each Raman mode.

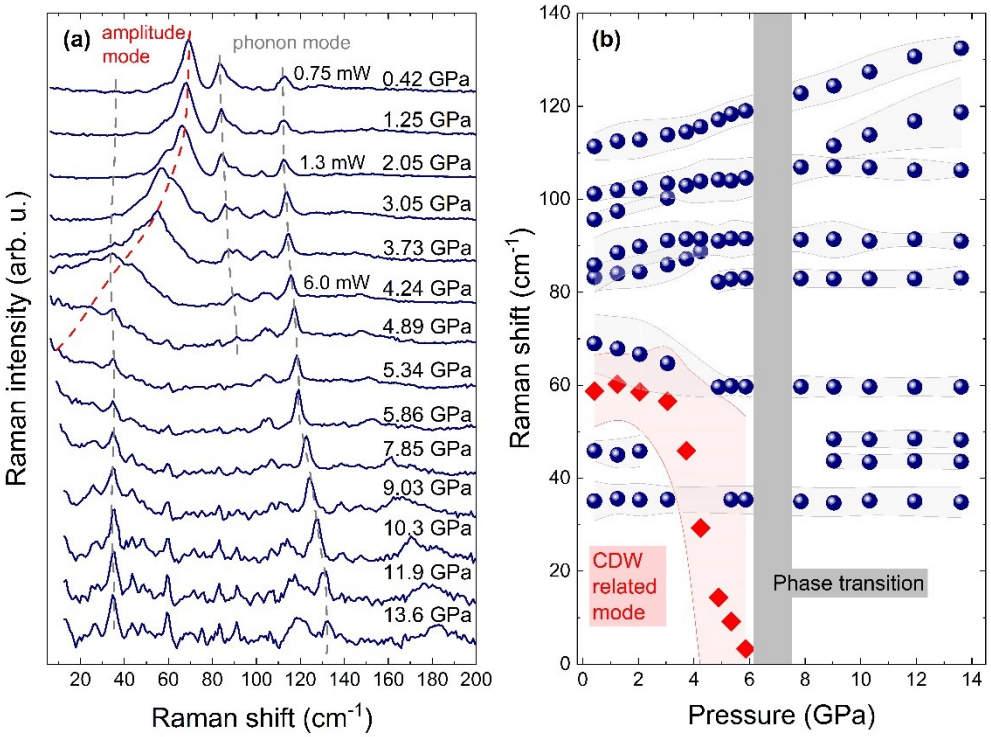


Figure S6. (a) Pressure-dependent Raman spectra obtained for $PrTe_3$ crystal (dashed lines are added as an eye guide). (b) Position of a phonon (navy points) and amplitude (red diamonds) mode in the function of pressure obtained with Lorentz fitting procedure – the shaded area represents broadening of each Raman mode.

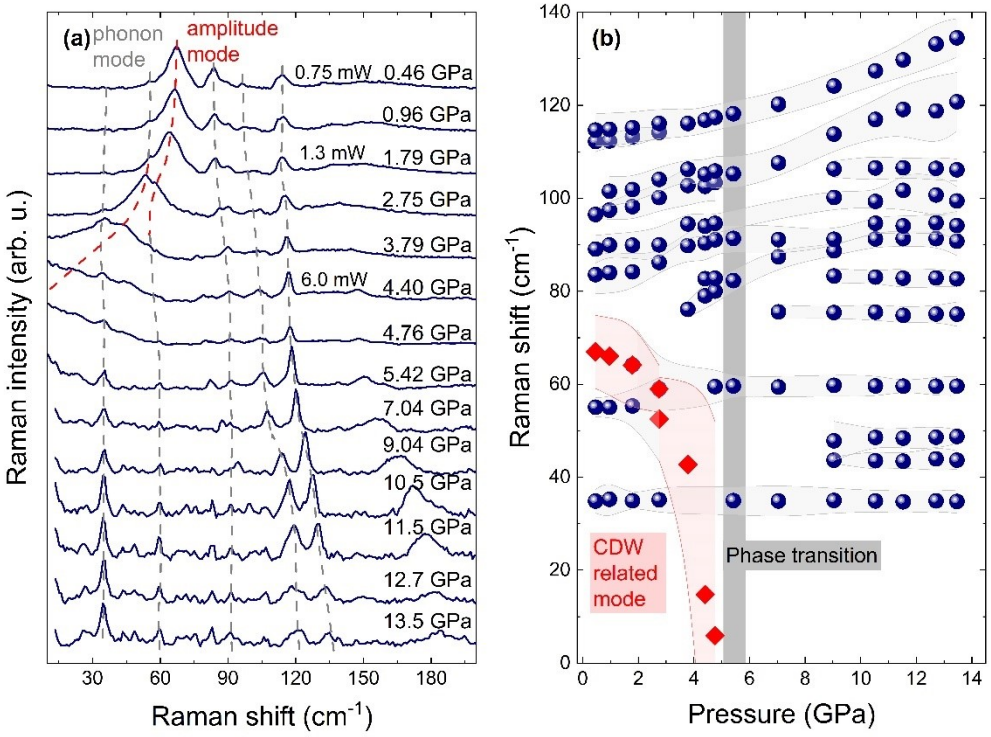


Figure S7. (a) Pressure-dependent Raman spectra obtained for $NdTe_3$ crystal (dashed lines are added as an eye guide). (b) Position of a phonon (navy points) and amplitude (red diamonds) mode in the function of pressure obtained with Lorentz fitting procedure – the shaded area represents broadening of each Raman mode.

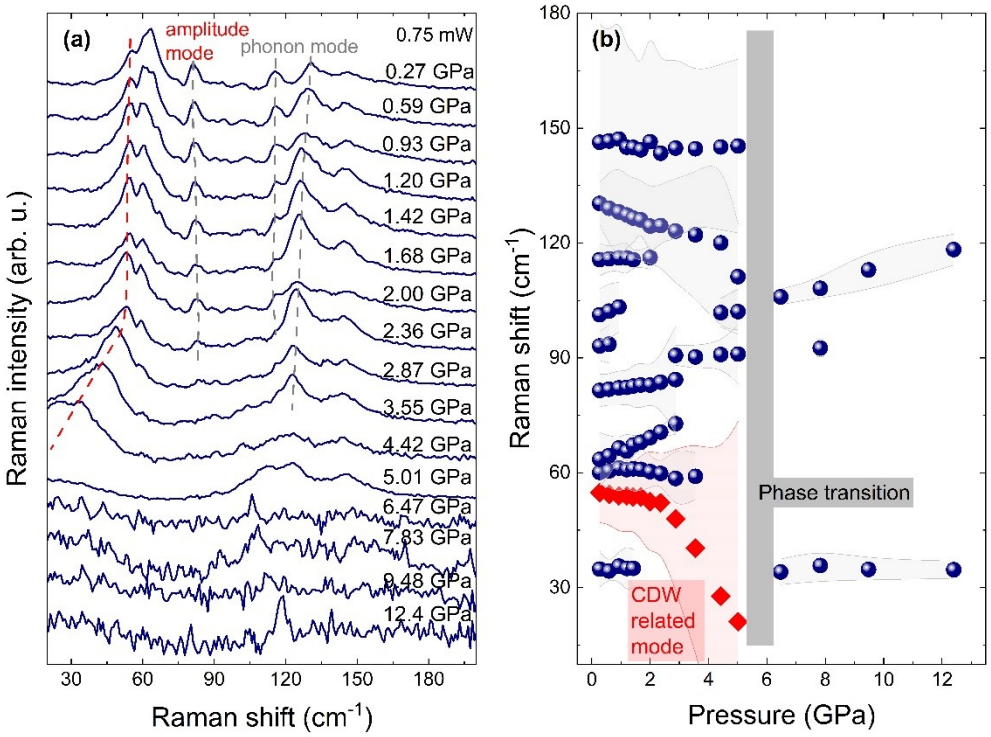


Figure S8. (a) Pressure-dependent Raman spectra obtained for $SmTe_3$ crystal (dashed lines are added as an eye guide). (b) Position of a phonon (navy points) and amplitude (red diamonds) mode in the function of pressure obtained with Lorentz fitting procedure – the shaded area represents broadening of each Raman mode.

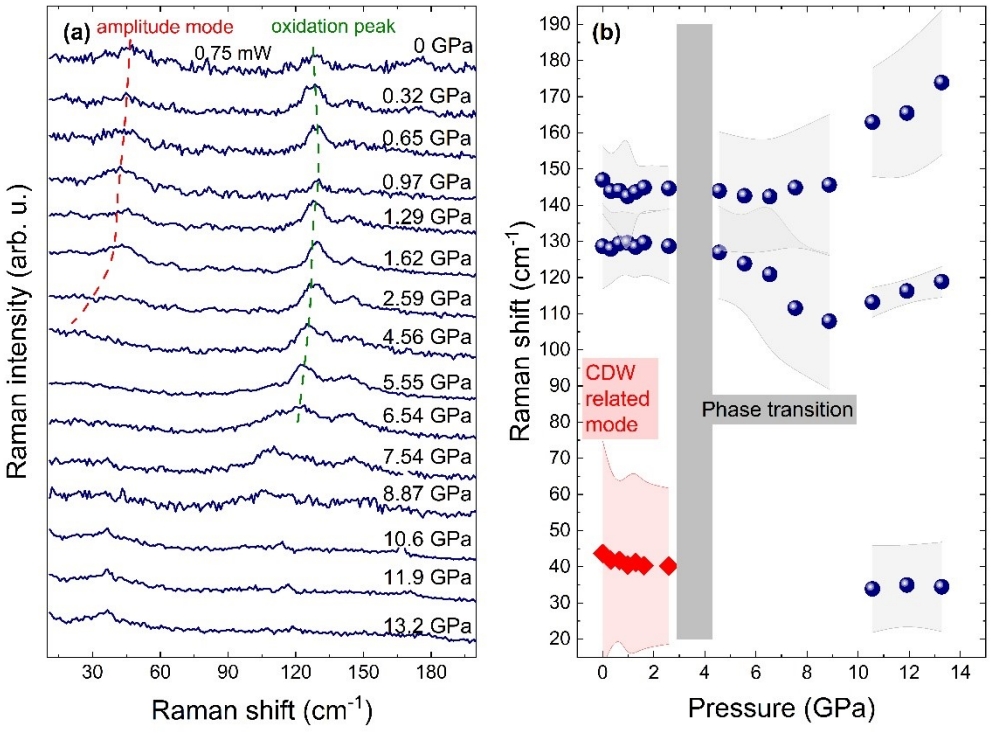


Figure S9. (a) Pressure-dependent Raman spectra obtained for $GdTe_3$ crystal (dashed lines are added as an eye guide). (b) Phonon (navy points) and amplitude mode (red diamonds) position in the function of pressure obtained with Lorentz fitting procedure – the shaded area represents broadening of each Raman mode.

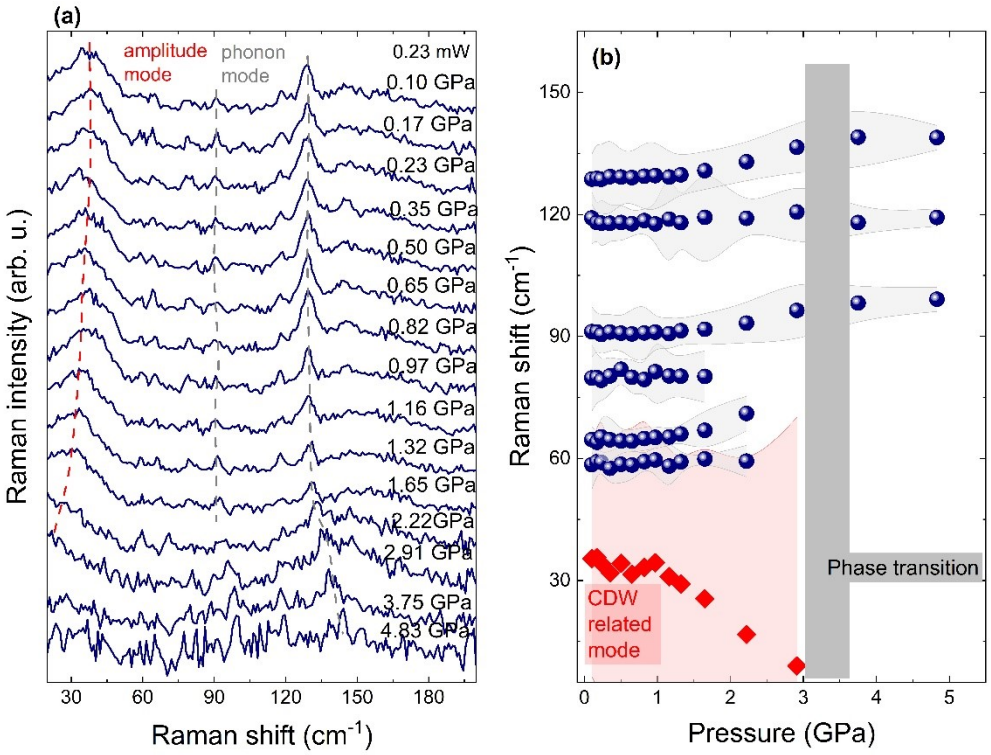


Figure S10. (a) Pressure-dependent Raman spectra obtained for $TbTe_3$ crystal (dashed lines are added as an eye guide). (b) Position of a phonon (navy points) and amplitude (red diamonds) mode in the function of pressure obtained with Lorentz fitting procedure – the shaded area represents broadening of each Raman mode.

## II. Angle-resolved Raman spectra obtained for $NdTe_3$ at 0, 1.97, and 12.43 GPa

This section shows the polar plot of Raman peak intensity for all modes observed for $NdTe_3$ crystals.

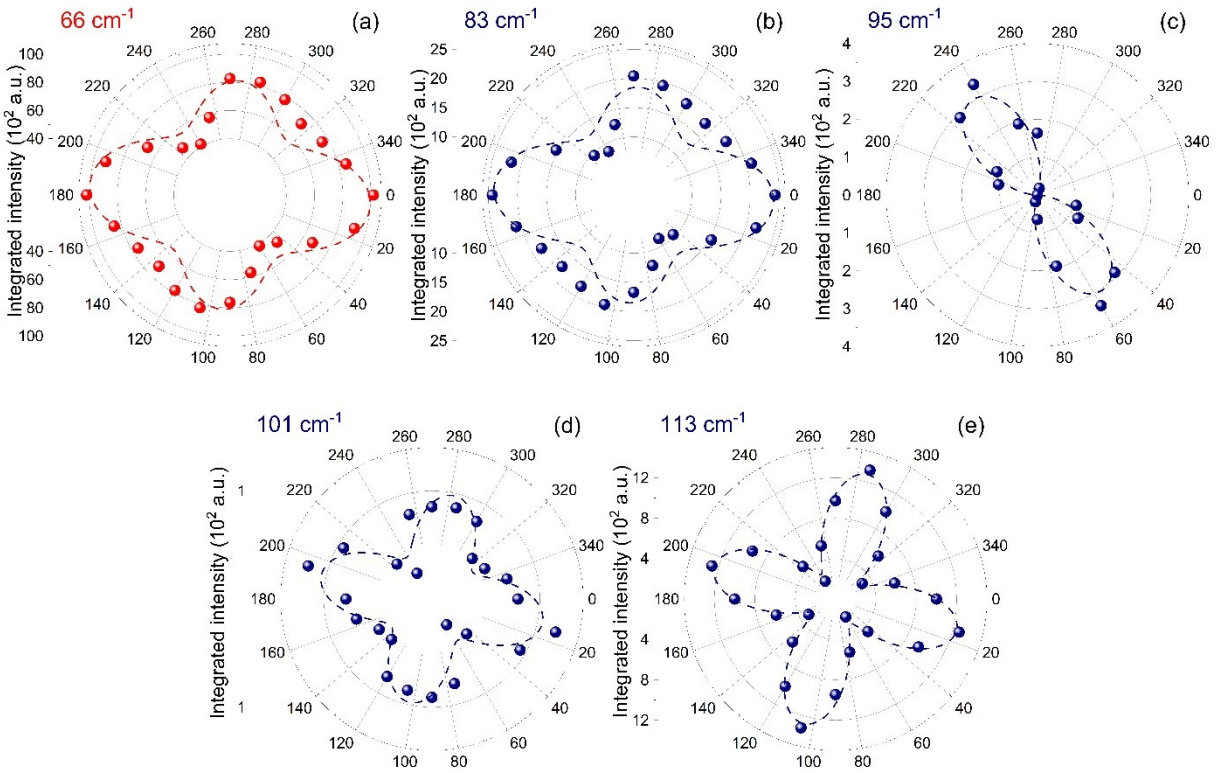


Figure S11. The polar plot of the integrated intensity of phonon mode: (a) 65 $cm^{-1}$, (b) 83 $cm^{-1}$, (c) 95 $cm^{-1}$, (d) 102 $cm^{-1}$, and (e) 113 $cm^{-1}$ obtained at 0 GPa for $NdTe_3$.

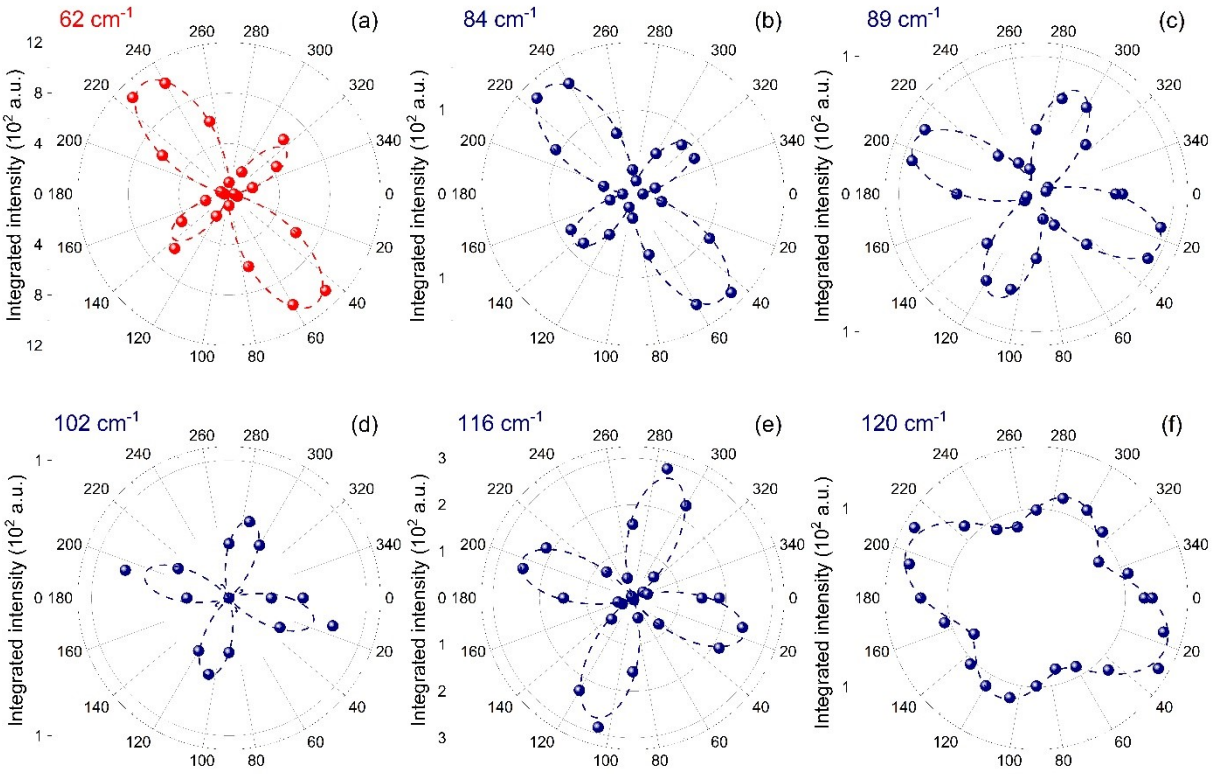


Figure S12. The polar plot of the integrated intensity of phonon mode: (a) 62 $cm^{-1}$, (b) 84 $cm^{-1}$, (c) 89 $cm^{-1}$, (d) 102 $cm^{-1}$, (e) 116 $cm^{-1}$, and (f) 120 $cm^{-1}$ obtained at 1.97 GPa (a) - (e) and 12.43 GPa (f) for $NdTe_3$.

## References


1 R. V. Yusupov, T. Mertelj, J.-H. Chu, I. R. Fisher and D. Mihailovic, *Phys. Rev. Lett.*, 2008, **101**, 246402.

2 M. Lavagnini, H.-M. Eiter, L. Tassini, B. Muschler, R. Hackl, R. Monnier, J.-H. Chu, I. R. Fisher and L. Degiorgi, *Phys. Rev. B*, 2010, **81**, 081101.

3 Y. Chen, P. Wang, M. Wu, J. Ma, S. Wen, X. Wu, G. Li, Y. Zhao, K. Wang, L. Zhang, L. Huang, W. Li and M. Huang, *Appl. Phys. Lett.*, 2019, **115**, 151905.